NETWORKS AND HETEROGENEOUS MEDIA
©American Institute of Mathematical Sciences
Volume **10**, Number **2**, June **2015**
doi:10.3934/nhm.2015.10.401
pp. **401–419**

# SELF-SIMILAR CONTROL SYSTEMS AND APPLICATIONS TO ZYGODACTYL BIRD'S FOOT

Anna Chiara Lai and Paola Loreti

Dipartimento di Scienze di Base e Applicate per l'Ingegneria
Sapienza Università di Roma
Via Antonio Scarpa 16
00161 Roma, Italy

(Communicated by Benedetto Piccoli)

Abstract. We investigate a class of linear discrete control systems, modeling the controlled dynamics of planar manipulators as well as the skeletal dynamics of human fingers and bird's toes. A self-similarity assumption on the phalanxes allows to reinterpret the control field ruling the whole dynamics as an Iterated Function System. By exploiting this relation, we apply results coming from self-similar dynamics in order to give a geometrical description of the control system and, in particular, of its reachable set. This approach is then applied to the investigation of the zygodactyl phenomenon in birds, and in particular in parrots. This arrangement of the toes of a bird's foot, common in species living on trees, is a distribution of the foot with two toes facing forward and two back. Reachability and grasping configurations are then investigated. Finally an hybrid system modeling the owl's foot is introduced.

1. **Introduction.** The aim of this paper is to introduce a class of linear discrete control systems, modeling the controlled dynamics of planar manipulators as well as the skeletal dynamics of human fingers and bird's toes. The key idea is to model robotic, human, avian finger as a sequence of links, whose relative (planar) angle is controlled by a discrete control function with values in a compact set. The main assumption regards the lengths $l_k$ of the links: they are assumed to decay according to a recursive and contractive relation, e.g. a constant scaling: $l_k = l_{k-1}/\rho$ with $\rho > 1$. We show that the recursively of the scaling relation, as well as its contractivity, allows to reinterpret the control field ruling the whole dynamics as an Iterated Function System, namely a set of contractive maps. This opens the way to the wide theoretical background of fractal geometry and, in particular, to the branch devoted to the investigation of self-similar structures. By establishing a relation between discrete control systems and fractals, well-known concepts and results coming from self-similar dynamics (like the attractor of an iterated function systems or the celebrated Open Set Condition) are used to describe the topology of the reachable set and other properties of the dynamical systems – see for instance [9] for an investigation on the left invertibility of discrete control systems via Iteration Function Systems.

2010 *Mathematics Subject Classification.* Primary: 58F12, 93A30; Secondary: 92B05.
*Key words and phrases.* Discrete control theory, iterated function systems, avian feet, zygodactyl feet, planar manipulator.

This approach was also explored in [8] and in [15], for a particular class of self-similar structures related to the theory of expansions in non-integer bases. The main novelty of this paper consists in the increased generality of the (linear) dynamics taken into account.

In the first part of the paper we shall focus on the study of the *asymptotic reachable set* of the manipulator, which in the first stage of our investigation is assumed to composed by a possibly infinite number of links, namely to belong to the class of so-called *hyper-redundant manipulators* – the term was introduced in [6] and it refers to manipulators with an high or possibly infinite kinematic redundancy. The interest of researchers in devices with hyper-redundant controls was motivated by the ability to avoid obstacles and the ability to perform new forms of robot locomotion and grasping (see for instance [1], [5] and [7]).

In the second part of the paper, an application to skeletal biology is showed: we assume the number of links to be *finite* and we investigate of the zygodactyl phenomenon in bird's feet. This arrangement of the toes of a bird's foot, common in species living on trees and in particular in parrots, is a distribution of the foot with two toes facing forward and two back. We apply the general self-similar model to the foot and we provide an algorithm computing the reachability set. Then we investigate the grasping problem, by providing sufficient, explicit conditions for the grasp of a branch, modeled as a cylinder. In general, our model may allow several grasping configurations: we adapt from robotics an optimality condition, maximizing the resistance of the grasp to external forces. Finally we introduce a hybrid dynamical system modeling owl's foot in various stages of hunting (flying, attack, grasp).

Biomechanics of avian foot, in particular in the case of arboreal birds, is widely investigated in the literature. We refer to [21] and the references therein for a discussion on the mechanics and energetics of trunk climbing and grasping of the treecreeper. In [4], Bock describes the morphology of woodpeckers and the biomechanical analysis of climbing and perching. Zinoviev and Dzerzhinsky, [27] studied the forces acting on avian limbs on various stages of locomotion, while Sustaita et al. [26] survey the tetrapod grasping in several clades, including birds. The above mentioned papers share a mechanical approach to the analysis of grasping and perching capabilities of avian feet: forces acting on bird's foot are described by considering in detail the whole skeleton-muscular system. Our model is a simplified version of these systems, on the other hand the dynamical system we consider is indeed a control system: this yields the possibility of investigating at once all the physically reasonable configurations of the foot.

The discrete control theoretic approach in the investigation of limb's kinematics is common in robotics - among many others, we refer to the papers [11], [17], [16] for an overview on robotic fingers that are investigated in a fashion similar to the one proposed in the present paper. Finally we note that the connection between the biomechanics of avian feet and robotics is an active research domain, mostly motivated by the fact that the locomotion of birds turned out to be more efficient with respect with human locomotion - see for instance the project described in [18], where the locomotion of birds is mimicked in a robotic device.

## 2. **Preliminaries: Iterated function systems and discrete control systems.**

The main point of this investigation is establish a relation in the linear case between the theory of Iterated Function Systems (IFSs) and a particular class of discrete

control problems. In particular, we aim to reinterpret the reachable set of a contractive discrete control system as the attractor of a suitable iterated function system, in a sense that is made clear below. In what follows we recall some basic facts about Iterated Function Systems and we establish a general relation with a class of discrete control models.

2.1. **Iterated function systems.** Iterated Function Systems are one of the main theoretical tools used to construct fractals and self-similar structures. In order to keep this introduction session as general as possible we shall set definitions and main results in a general metric space $(X, d)$. However, our applications are mainly concerned with the $n$-dimensional complex field $\mathbb{C}^n$, or, in some cases, to its isomorphic space $\mathbb{R}^{2n}$. IFSs are collections of *contractive maps* $(F_u)_{u\in U}$ and, as one may expect, their main features are related to fixed point arguments. We recall that a function in a metric space $(X, d)$ is a *contraction*, if for every $x, y \in X$

$$d(F(x), F(y)) \leq Ld(x, y)$$

for some $L < 1$. Every IFS is naturally associated with the so called *Hutchinson operator*, a set-valued map defined by

$$\mathcal{F}(S) := \bigcup_{u\in U} F_u(S).$$

By definition $\mathcal{F}$ acts of the power set of $X$, $P(X)$. $P(X)$ is a metric space, as well, if it is endowed with the *Hausdorff distance* $d_H$ induced by the distance of $X$:

$$d_H(A, B) := \max\{\sup_{b\in B}\inf_{a\in A} d(a, b), \sup_{a\in A}\inf_{b\in B} d(a, b)\}.$$

Hutchinson [10] showed that every finite IFS, namely every IFS with finitely many contractions, admits a unique non-empty compact fixed point $Q$. In other words, there exists and it is unique a compact subset $R$ of $X$ such that

$$Q = \mathcal{F}(Q).$$

Moreover $Q$ is also an *attractor* for $\mathcal{F}$: for every non-empty bounded set $S \subseteq X$

$$\lim_{k\to\infty} \mathcal{F}^k(S) = Q.$$

This result was lately generalized to the case of infinite *bounded* IFSs ([25] and [19]). Let $(F_u)_{u\in U}$ be an IFS and for every $u \in U$ denote by $L_u$ the Lipschitz constant of $F_u$. Then $(F_u)_{u\in U}$ is *bounded* if $(L_u)_{u\in U}$ is uniformly bounded from above by a constant $c < 1$, i.e., if

$$c := \sup_{u\in U} L_u < 1.$$

The attractor $Q$ of an IFS can be characterized by means of the associated *shift space* $U^\infty$, the space of infinite sequences of element of the index set $U$. Indeed one has that for every bounded subset $S$ of $X$

$$Q = cl\left(\left\{\lim_{k\to\infty} F_{u_1} \circ F_{u_2} \circ \cdots \circ F_{u_k}(S) \mid (u_1, \ldots, u_k, \ldots) \in U^\infty\right\}\right) \tag{1}$$

where $cl(S) = \overline{S}$ denotes the closure of a set $S$.

**Example 1.** Consider the simple IFS given by $F_u : x \mapsto \frac{1}{\rho}(x + u)$ with $\rho > 1$ and $u \in U$, where $U$ is a compact subset of $\mathbb{R}$. Then by a direct computation

$F_{u_1} \circ \cdots \circ F_{u_k}(0) = \sum_{j=1}^{k} u_j \rho^{-j}$. By applying (1) with $S = \{0\}$ we obtain that the attractor of $(F_u)$ is

$$Q = \left\{ \sum_{j=1}^{\infty} u_j \rho^{-j} \mid (u_j) \in U^{\infty} \right\}.$$

As we shall see in next sections, the reachable set of some control problems can be identified with the attractor of suitable IFSs: the key idea is to see the (contractive) controlled dynamics $F(\cdot, u)$ of a control system $\dot{x} = F(x, u)$ as an element of an IFS. In the next section, this relation is described in a detailed way for a particular class of control systems; here we are interested to keep the argument at a more intuitive level. The controls $u$ are encoded as the indexes of the functions of the IFS, so that $F(\cdot, u) = F_u(\cdot)$. Borrowing the content of above example, we can keep in mind as a toy model the following discrete control system

$$x_k = \frac{1}{\rho}(x_{k-1} + u_k) \quad u_0 = 0,\ u_k \in U. \tag{2}$$

The velocity field of above system is $F_u(x) = \frac{1}{\rho}(x + u)$ and we may store this information with the formalism of IFSs by considering the family of contractive maps $(F_u)_{u \in U}$. Given a control sequence $\bar{u} = (u_k) \in U^{\infty}$, the associated trajectory $(x_k[\bar{u}])$ satisfies for every $k \geq 1$

$$x_k = F_{u_k} \circ \cdots \circ F_{u_1}(0) = \sum_{j=1}^{k} u_{k-j} \rho^{-j}.$$

Note that the above relation is backward in time with respect to the control $\bar{u}$. However when we consider the *reachable set* in time $k$ we get

$$R_k := \{x_k[\bar{u}] \mid \bar{u} \in U^{\infty}\} = \{\sum_{j=1}^{k} u_{k-j} \rho^{-j} \mid \bar{u} \in U^{\infty}\} = \{\sum_{j=1}^{k} u_j \rho^{-j} \mid \bar{u} \in U^{\infty}\}.$$

Using IFS formalism and considering the Hutchinson operator $\mathcal{F}$ associated to $(F_u)_{u \in U}$ we get

$$R_k = \mathcal{F}^k(\{0\}). \tag{3}$$

When considering the attractor $Q$ of $\mathcal{F}$, described explicitly in above example, the *asymptotic* reachable set $R_\infty$ of this system satisfies

$$R_\infty := \{ \lim_{k \to \infty} x_k[u] \mid u \in U^{\infty}\} = \lim_{k \to \infty} R_k = \lim_{k \to \infty} F^k(\{0\}) = Q.$$

More generally, the iteration of an IFS via the Hutchinson operator can be reinterpreted as a discrete time evolution of a control system. The attractor, namely the set of the possible outcomes of infinite iterations of the controlled velocity maps, is naturally associated to the asymptotic reachable set.

Fractal geometry is a theoretical framework providing a description of the topology of the attractor and, consequently, of the reachable set of some discrete control systems. For instance, in the case of finite IFS over $\mathbb{R}^n$, we may consider the celebrated *Open Set Condition* (OSC), stating that there exists a relatively compact open set $V \subset \mathbb{R}^n$ such that $\mathcal{F}(V) \subset V$ and that the images $F_u(V)$, with $u \in U$, are disjoint. If this condition is satisfied then the attractor has a positive Hausdorff dimension $s$, that can be explicitly calculated by solving the equation $1 = \sum_{u \in U} L_u^s$, where $L_u$ denotes the Lipschitz constant of the map $F_u$ [10]. In the case of *coformal* finite IFS, the conversely was proved to be also true [23].

**Example 2.** Consider the control system (2) control set $U = \{0, 1\}$. The OSC on $(F_u)$ is satisfied if and only if $\rho > 2$. If $\rho > 2$ then asymptotic reachable set has Hausdorff dimension $\log_2 \rho$. In particular, $R_\infty$ is a totally disconnected set. Note that for $\rho = 3$ we obtain a scaled version of the Middle Third Cantor set.

The parallelism between discrete control dynamics and IFS can be extended to the investigation of the uniqueness of the controlled trajectories, whose relevance has twofold motivations. When there is a one-to-one relation between control and trajectory, then observability properties emerge or, with the terminology coming from engineering, we can say that the system is *reversible* or *invertible* – see [9] for an investigation of this issue via IFS.

On the other hand, a redundancy of the trajectories naturally opens questions about optimality with respect to a given running cost. The theory of IFS is a fertile framework also for this kind of problems: we refer to Barnsley's book [2] for a general overview on the topic. We finally remark that a wide literature was devoted for the unidimensional linear case, as a branch of the theory of expansions in non-integer bases, see for instance [14], [12], [22], [13] and references therein.

2.2. **Affine IFS.** In this paper we are interested on a particular class of affine IFSs on $\mathbb{C}^n$, whose maps are of the form

$$F_u(x) = e^{-i\omega u}(Ax + B) \tag{4}$$

for some contractive linear operator $A : \mathbb{C}^n \to \mathbb{C}^n$, $B \in \mathbb{C}^n$, $\omega \in [0, 2\pi)$ and $u \in U \subset \mathbb{R}$. Note that $F_u$ is composed by a "controlled" rotation term $e^{-i\omega u}$ and a fixed contraction-displacement term $Ax + B$.

By construction, $(F_u)_{u\in U}$ is a bounded IFS. Indeed for all $u \in U$ one has $L_u = ||A||$, where $||A||$ is the essential norm of $A$, defined by

$$||A|| := \sup_{x\in\mathbb{C}^n, ||x||\leq 1} ||Ax|| < 1. \tag{5}$$

The last inequality is given by the fact that we assumed above $A$ to be contractive. In order to give an explicit description of the attractor $R$ of $(F_u)_{u\in U}$, we note that for every $u, v \in U$

$$F_u \circ F_v(0) = e^{-i\omega(u+v)}AB + e^{-i\omega u}B.$$

By iteratively applying above equality, for every sequence $(u_k) \in U^\infty$ one has

$$\lim_{k\to\infty} F_{u_1} \circ \cdots F_{u_k}(0) = \sum_{k=1}^{\infty} e^{-i\omega \sum_{h=1}^{k} u_k} A^{k-1}B.$$

Finally, by taking $S = \{0\}$ in (1), we obtain

$$Q = \left\{ \sum_{k=1}^{\infty} e^{-i\omega \sum_{h=1}^{k} u_h} A^{k-1}B \mid (u_k) \in U^\infty \right\}. \tag{6}$$

For our purposes we shall take into account matrices $A$ whose spectral radius $\rho(A) < 1$. This is a milder assumption than (5), but in general if $\rho(A) < 1$ then there exists $K \geq 1$ such that for every $k \geq K$ one has $||A^k|| < 1$. For this reason we shall also refer to such operators as *eventually contractive*. Clearly $Q$, as it is given in (6), is well defined even in the case of eventually contractive IFSs of the form (4). By a direct computation, one can convince himself that $R$ is an invariant set for the associated Hutchinson operator. Indeed, next results shows that $Q$ is the *unique* compact invariant set for the class of eventually contractive IFSs.

**Proposition 1.** *Let $A$ be a complex-valued $n \times n$ matrix with $\rho(A) < 1$, $B \in \mathbb{C}^n$, $U \subset \mathbb{R}$ and $\omega \in [0, 2\pi)$. Consider the eventually contractive IFS*

$$F_u(x) := e^{-i\omega u}(Ax + B).$$

*Then*

$$Q = \left\{ \sum_{k=1}^{\infty} e^{-i\omega \sum_{h=1}^{k} u_k} A^{k-1} B \mid (u_k) \in U^{\infty} \right\}$$

*is the unique invariant set for $(F_u)_{u\in U}$. Moreover for every bounded set $S$*

$$\lim_{k\to\infty} \mathcal{F}^k(S) = Q$$

*where $\mathcal{F}$ is the Hutchinson operator associated to $(F_u)_{u\in U}$.*

*Proof.* As mentioned above, the invariance of $Q$ follows by a direct computation. To show its uniqueness, let $K$ be the smallest integer such that $||A^k|| < 1$ for every $k \geq K$. Also consider the space $U^K$ of sequences in $U$ of length $K$ and an auxiliary IFS composed by the contractive maps:

$$F_{u_1,\dots,u_K} := F_{u_1} \circ \cdots \circ F_{u_K}$$

For brevity we denote the index sequence $u_1, \dots, u_K$ by $\bar{u}$, so that the above IFS also reads $(F_{\bar{u}})_{\bar{u}\in U^K}$.

Now, let $Q'$ be an invariant for $(F_u)_{u\in U}$, the original eventually contractive IFS. Then $\mathcal{F}(Q') = Q'$ and, consequently, $\mathcal{F}^{Kh}(Q') = Q'$, for every $h \in \mathbb{N}$. But

$$\mathcal{F}^{Kh}(\cdot) = \bigcup_{u_1,\dots,u_{Kh}\in U} F_{u_1} \circ \cdots \circ F_{u_{Kh}}(\cdot) = \bigcup_{\bar{u}^1,\dots,\bar{u}^h\in U^K} F_{\bar{u}^1} \circ \cdots \circ F_{\bar{u}^h}(\cdot).$$

Then $Q'$ is an invariant set for the IFS $(F_{\bar{u}})_{\bar{u}\in U^K}$, too. Therefore, since compact invariant sets for purely contractive, classical IFSs are unique ([10] and [25]), the same holds in the eventually contractive case. To complete the proof it is left to prove that for every bounded set $S$ the already established limit

$$\lim_{h\to\infty} \mathcal{F}^{hK}(S) = Q$$

(if follows by the fact that $\mathcal{F}^K$ is a contractive IFS) implies

$$\lim_{k\to\infty} \mathcal{F}^{k}(S) = Q.$$

We notice that $\mathcal{F}$ is uniformly continuous (see [3] for an overview on the continuity of $\mathcal{F}$). Consequently for every $m \in \mathbb{N}$ and for every $\varepsilon > 0$ there exists $\delta_m > 0$ such that

$$d_H(S_1, S_2) < \delta_m \quad \Rightarrow d_H(\mathcal{F}^m(S_1), \mathcal{F}^m(S_2)) < \varepsilon.$$

Fix $\varepsilon > 0$, and let $H$ be such that

$$d_H(\mathcal{F}^{Kh}(S), Q) < \delta_m \qquad \forall h \geq H,\ m = 1, \dots, K.$$

For every $k > KH$ we may write $k = Kh + m$ for some $h \geq H$ and some $m = 1, \dots, K$. Therefore we finally get

$$d_H(\mathcal{F}^{Kh+m}(S), Q) = d_H(\mathcal{F}^m(F^{Kh}(S)), \mathcal{F}^m(Q)) < \varepsilon$$

and this concludes the proof. □

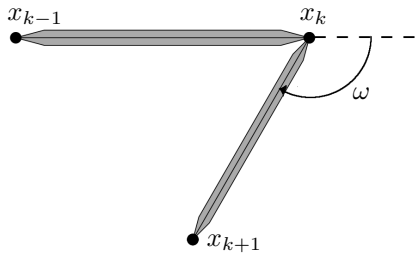


FIGURE 1. In this figure the $k+1$-th rotation control $v_{k+1}$ is equal to 1: this corresponds to rotate the $k+1$-th phalanx, whose junctions are $x_k$ and $x_{k+1}$ of an angle $\omega$ with respect to the $k$-phalanx.

3. **Discrete control systems for skeletal motion.** Throughout this section we introduce a simple control model describing the kinematics of a sequence of rigid links whose relative angles can be controlled by actuators on the junctions. Note that this approach applies to robotics, where a sequence of mobile rigid links is termed *manipulator*, as well as to skeletal biology. As an example of applications, in the next sections we shall focus on the kinematics of the avian foot and we shall also consider the interplay between couples of bird fingers.

In order to build our model, consider a sequence of one-dimensional links of length $l_k$, $k \in \mathbb{N}$. We denote by $x_k$ and $x_{k+1}$ the positions of the endpoints (junctions) of the $k$-th link. We assume the motion of the links to be planar and, since rotations are involved, it is more comfortable to set our dynamics on the complex plane, so that $x_k \in \mathbb{C}$. Finally every junction $x_k$ is endowed a rotation control $u_k$ belonging to a compact control set $U \subset \mathbb{R}$. We finally introduce a maximal rotation $\omega \in [0, 2\pi]$, so that the effective clockwise rotation of the $k$-th link with respect to the former can be described by $-\omega u_k$. For instance if $u_k = 0$ then the $(k-1)$-th and the $k$-th links are collinear, while if $u_k = 1$ then a rotation of amplitude $\omega$ is applied and, consequently, the $(k-1)$-th and the $k$-th links form an angle $\pi - \omega$, see Figure 1. In view of above reasoning, we may assume without loss of generality $U \subset [0, 1]$. Summarizing, one has for every $k$

$$||x_k - x_{k-1}|| = l_k \qquad arg(x_k - x_{k-1}) = arg(x_{k-1}) - \omega u_k. \tag{7}$$

By iteratively applying last equality (and by setting $arg(x_0) := 0$) we obtain $x_k - x_{k-1} = l_k e^{-i\omega \sum_{h=1}^{k} u_h}$. Setting as initial datum $x_0 = 0$, we finally get the discrete control system

$$\begin{cases} x_k = x_{k-1} + l_k e^{-i\omega \sum_{h=1}^{k} u_h} \\ x_0 = 0 \qquad u_k \in U,\ k \in \mathbb{N}. \end{cases} \tag{8}$$

For every control sequence $\bar{u} = (u_1, \dots, u_k, \dots) \in U^\infty$, the trajectories $x_k[\bar{u}] = x_k$ of above system are given by

$$x_k = \sum_{j=1}^{k} l_j e^{-i\omega \sum_{h=1}^{j} u_h}, \qquad k \in \mathbb{N}.$$

Then we may explicitly write the *reachable set in time k*

$$R_k := \{x_k[\bar{u}] \mid \bar{u} \in U^\infty\} = \left\{ \sum_{j=1}^{k} l_j e^{-i\omega \sum_{h=1}^{j} u_h} \mid u_1, \dots, u_k \in U \right\}. \tag{9}$$

Finally, we note that if the sequence of link lengths $(l_k)$ is summable, then the *asymptotic reachable set* $R_\infty := \lim_{k\to\infty} R_k$ is a compact set:

$$R_\infty = \left\{ \lim_{k\to\infty} x_k[\bar{u}] \mid \bar{u} \in U^\infty \right\} = \left\{ \sum_{j=1}^{\infty} l_j e^{-i\omega \sum_{h=1}^{j} u_h} \mid u_1, \dots, u_k \in U \right\}. \tag{10}$$

3.1. **Asymptotic reachability for self-similar links.** We noticed above that the notion of asymptotic reachable set makes sense under an obvious finiteness condition of the total length of the links, namely $\ell := \sum_{k=1}^{\infty} l_k < +\infty$. Among all the summable sequences, we take into account the class of positive sequences $(l_k)$ that can be recursively generated via a contractive, linear transformation. We shall see that this assumption allows to reinterpret the asymptotic reachable set as the attractor of a suitable IFS.

**Definition 3.1.** We say that a sequence $(l_k)$ in $\mathbb{R}$ is Linear-Contractive-Recursive (LCR) if there exist an integer $n \in \mathbb{N}$ and a linear map $f : \mathbb{R}^n \to \mathbb{R}$ satisfying $l_k = f(l_{k-1}, \dots, l_{k-n})$ for every $k > n$ and there exists $L < 1$ such that

$$|f(x) - f(y)| < L||x - y||_\infty \tag{11}$$

where $||(x_1, \dots, x_n)||_\infty := \max\{|x_k|, k = 1, \dots, n\}$ denotes the $L^\infty$-norm of $x \in \mathbb{R}^n$.

A trivial example of linear-contractive-recursive (LCR) sequence is given by the geometric sequence $l_k = q^{-k}$ for some $q > 1$. Indeed $l_k = l_{k-1}q^{-1}$ for every $k \in \mathbb{N}$. An other example consists in the scaled Fibonacci sequence $l_k = \tilde{F}_k q^{-k}$. Here $q$ is assumed greater than the Golden Mean $\varphi$ and $\tilde{F}_{k+1} = \tilde{F}_{k-1} + \tilde{F}_k$ denotes the $k$-th Fibonacci number. Indeed one has

$$l_k = l_{k-1}q^{-1} + l_{k-2}q^{-2}, \qquad \forall k \geq 2.$$

**Remark 1.** Generating functions of LCR sequences are always contractions with respect the Euclidean norm $||\cdot||$, while the conversely is not necessarily true whenever $n \geq 2$. This immediately follows by the inequality

$$||x||_\infty \leq ||x|| \quad \forall x \in \mathbb{R}^n.$$

To make clearer above definition, observe that by definition the scaled Fibonacci sequence $\tilde{F}_k q^{-k}$ is LCR if and only if $q > \varphi$, while the generating map $f(x, y) = xq^{-1} + yq^{-2}$ is a contraction with respect Euclidean norm if and only if $q > \sqrt{\varphi}$. Finally notice that the series $\sum \tilde{F}_k q^{-k}$ converges if and only if $q > \varphi$ ( and not if $q > \sqrt{\varphi}$). This fact is clarified in the next proposition.

**Proposition 2.** *LCR sequences are summable.*

*Proof.* Let $(l_k)$ be a LCR sequence and let $L < 1$ be the $L^\infty$- Lipschitz constant of its generating function $f : \mathbb{R}^n \to \mathbb{R}$. Then for every $k > n$ one has

$$|l_k| \leq L|(l_{k-1}, \dots, l_{k-n})|_\infty = L|l_{k'}|$$

where $l_{k'} := \max\{l_{k-1}, \dots, l_{k-n}\}$. By iteratively applying the above inequality we have

$$|l_k| \leq L^k \qquad \forall k \geq n. \tag{12}$$

Note that this inequality is sharp when $k' = k-1$ for all $k$, as in the case of scaled-Fibonacci sequence. The claim hence follows by the comparison between the series $\sum_{k>n} |l_k|$ and the geometric series $\sum_{k>n} L^k$. □

In order to investigate the reachability properties of the control system (8), we fix a LCR sequence $(l_k)$. In what follows we build an eventually contractive IFS naturally associated to $(l_k)$. To this end, recall that the dual of $\mathbb{R}^n$ is isomorphic to $\mathbb{R}^n$ itself, that is every linear map from $f : \mathbb{R}^n \to \mathbb{R}$ can be identified with an element $a \in \mathbb{R}^n$. In other words, there exists $a = (a_1, \dots, a_n) \in \mathbb{R}^n$ such that for every $k > n$

$$l_k = \langle a, (l_{k-1}, \dots, l_{k-n}) \rangle.$$

Note that since $(l_k)$ is LCR, and in particular the $L^\infty$-Lipschitz constant of $f$ is smaller than 1, then

$$||a||_1 := \sum_{k=1}^{n} |a_k| < 1. \tag{13}$$

**Remark 2.** Above inequality is an application of Hölder inequality in the finite-dimensional case. However a more direct proof consists in setting for all $j = 1, \dots, n$

$$x_j = \begin{cases} |a_j|/a_j & \text{if } a_j \neq 0 \\ 0 & \text{otherwise} \end{cases}$$

and in applying Condition (11) to $x = (x_1, \dots, x_n)$ and to $y = 0_n := (0, \dots, 0) \in \mathbb{R}^n$.

Now, define the $n \times n$ matrix

$$A := \begin{pmatrix} a_1 \dots a_{n-1} & a_n \\ \mathbf{I}_{n-1} & 0_{n-1} \end{pmatrix}$$

where $\mathbf{I}_{n-1}$ denotes the $(n-1)$-dimensional identity matrix. By construction, for every $k > n$

$$A(l_{k-1}, l_{k-2}, \dots, l_{k-n})^T = (l_k, l_{k-1}, \dots, l_{k-n+1})^T, \tag{14}$$

that is $A$ acts on $(l_k)$ as a shift operator with window of length $n$.

So far we fixed a LCR sequence of lengths $(l_k)$ and we associated to it a $n$-dimensional eventually contractive linear operator $A$, describing the evolution of $(l_k)$ via (14). We now consider the eventually contractive affine IFS $(F_u)_{u \in U}$ defined on $\mathbb{C}^n$

$$F_u(x) := e^{-i\omega u}(Ax + B) \qquad u \in U. \tag{15}$$

where

$$B = (l_n, l_{n-1}, \dots, l_1)^T.$$

Note that by (14)

$$A^k B = (l_{k+n}, \dots, l_{k+1})^T \qquad \forall k > 0. \tag{16}$$

**Remark 3** (Spectral localization of $A$)**.** We notice that (16), together with (12), implies $\lim_{k\to\infty} ||A^k B||_\infty = 0$. Therefore $A^k$ tends to 0 as $k$ tends to infinity, and consequently, *the spectral radius of $A$ is strictly lower than* 1.

**Theorem 3.2.** *Let $\mathcal{F}(S) := \cup_{u \in U} F_u(S)$ be the Hutchinson operator associated to $(F_u)_{u \in U}$ and denote by $\pi_1$ the projection of a vector of $\mathbb{C}^n$ on its first component. Then for every $k \geq 0$, the reachable set in time $k$ of the control system (8), $R_k$, satisfies*

$$R_k = \pi_1 \mathcal{F}^k(\{0\}). \tag{17}$$

*Furthermore let $Q_\infty$ be the (unique) invariant set of $(F_u)_{u\in U}$. Then asymptotic reachable set $R_\infty$ satisfies*

$$R_\infty = \pi_1(Q_\infty)$$

*and for every bounded set $S \subset \mathbb{C}^n$*

$$R_\infty = \pi_1(\lim_{k\to\infty} \mathcal{F}^k(S)),$$

*Proof.* Let $Q_k := \mathcal{F}^k(\{0\})$. By (3) one has

$$Q_k = \left\{ \sum_{j=k}^{\infty} e^{-i\omega \sum_{h=1}^{j} u_h} A^{k-1} B \mid (u_k) \in U^\infty \right\}.$$

and, by (16) we may rewrite above equality as

$$Q_k = \left\{ \sum_{j=k}^{\infty} e^{-i\omega \sum_{h=1}^{j} u_h} (l_{n+k}, \dots, l_{k+1}) \mid (u_k) \in U^\infty \right\}.$$

Then (17) follows by noting that

$$R_k = \left\{ \sum_{j=k}^{\infty} e^{-i\omega \sum_{h=1}^{j} u_h} l_k \mid (u_k) \in U^\infty \right\} = \pi(Q_k).$$

By Proposition 1, the compact set $Q_\infty \subset \mathbb{C}^n$ is well defined an it satisfies

$$Q_\infty = \left\{ \sum_{k=1}^{\infty} e^{-i\omega \sum_{h=1}^{k} u_h} A^{k-1} B \mid (u_k) \in U^\infty \right\}.$$

Again by (16) we may rewrite above equality as

$$Q_\infty = \left\{ \sum_{k=1}^{\infty} e^{-i\omega \sum_{h=1}^{k} u_h} (l_{n+k-1}, \dots, l_k) \mid (u_k) \in U^\infty \right\}$$

so that one has by (10)

$$\pi_1(Q_\infty) = \left\{ \sum_{k=1}^{\infty} e^{-i\omega \sum_{h=1}^{k} u_k} l_k \mid (u_k) \in U^\infty \right\} = R_\infty.$$

Finally, the last part of the claim follows again by Proposition 1. □

**Example 3.** If $l_k = 1/\rho^k$ for all $k \geq 1$ (namely $l_0 = 1$) then $R_\infty$ is the attractor of the one-dimensional IFS on $\mathbb{C}$

$$F_u(x) = e^{-i\omega u} \frac{1}{\rho}(x+1)$$

If $l_k = F_k/\rho^k$ for all $k \geq 1$ (namely $l_0 = F_0$ and $l_1 = F_1/\rho$) then $R_\infty$ is the projection on the first component of the attractor of the two-dimensional IFS

$$F_u(x_1, x_2) = e^{-i\omega u} \begin{pmatrix} \frac{1}{\rho} & \frac{1}{\rho} \\ 1 & 0 \end{pmatrix} (x_1 + F_0, x_2 + F_1/\rho)^T.$$

Next result gives informations about the geometry of $R_\infty$ in the case of $l_k = 1/\rho^k$

**Corollary 1.** *Assume* $l_k = 1/\rho^k$ *for all* $k \geq 1$, $\rho > 2$ *and* $U = \{u_1, u_2\}$ *with* $\bar{u} := u_2 - u_1$ *satisfying*

$$\sqrt{1 - \cos(\omega \bar{u})} > \frac{1}{2\sqrt{2}}. \tag{18}$$

*Then* $R_\infty$ *has Hausdorff dimension equal to* $\log_\rho 2$ *and, consequently, it is a totally disconnected set.*

*Proof.* By Theorem 3.2 $R_\infty$ is the attractor of the IFS

$$F_u(x) = e^{-i\omega u}\frac{1}{\rho}(x+1) \quad u \in \{u_1, u_2\}.$$

It is left to show that $(F_u)$ satisfies the Open Set Condition (see Section 2.2), namely that there exists a open set $V$ such that

$$F_{u_1}(V) \cup F_{u_2}(V) \subseteq V. \tag{19}$$

and

$$F_{u_1}(V) \cap F_{u_2}(V) = \emptyset. \tag{20}$$

To this end set $V = B_1(0)$ the open unit ball on the complex plane, and note that if $\rho > 2$ then (19) is satisfied. To show (20), we observe that $F_{u_1}(V) \cap F_{u_2}(V)$ its the union of two balls of radius $r := \frac{1}{\rho}$ and whose centers are respectively $c_1 := e^{-i\omega u_1}$ and $c_2 := e^{-i\omega u_2}$. Then by (18) the distance between $c_1$ and $c_2$ satisfies

$$|c_1 - c_2| = \frac{\sqrt{2}}{\rho}\sqrt{1 - \cos(\omega \bar{u})} > \frac{r}{2}$$

and, consequently, (20) holds. Finally recall that when the OSC is satisfied the Hausdorff dimension $s$ is the solution of the equation

$$1 = 2\left(\frac{1}{\rho}\right)^s,$$

(indeed $\frac{1}{\rho}$ is the Lipschitz constant of $F_{u_1}$ and $F_{u_2}$) and this concludes the proof. □

4. **A model for zygodactyl bird's foot.** Zygodactyl bird's foot is composed by four pairwise opposable toes. It occurs parrots, woodpeckers, cuckoos and some owls. The arrangement of the fingers varies with species, we shall consider the case in which the motions of opposite finger are coplanar; see Figure 2 for an example.

Building our model consists into two stages: we first slightly modify the control system (8) in order to take into account several toes, we then consider the global arrangement of all the toes in a general three-dimensional setting. The rest of the paper is devoted to investigation of the grasping capabilities of feet and to the description of an hybrid dynamical system modeling the *tendon locking mechanism*, a feature of owl's (zygodactyl) feet.

4.1. **Bird's toes on the complex plane.** In previous section we introduced a model for a toe (or for a manipulator) on the complex plane, whose kinematics is ruled by control system (8) . In what follows, physical assumptions (planar motion, lengths $l_k$ are LCR sequences, maximal rotation angle $\omega$ is fixed) and control assumptions hold still. The corresponding control dynamics is a slight modification of (8), described below.

First of all we notice that, for simplicity, the reference frame of (8) is set in order to have $x_0 = 0$ and the axes oriented along the first link: the position of the first junction simply reads $x_1 = l_1 e^{-i\omega u_1}$, and $x_1$ belongs to the real axes if no rotation

is performed, i.e., if $u_1 = 0$. Since our goal is to model a whole foot, where several toes are involved, a general reference frame is needed. All the toes of the bird's foot are assumed to share the same initial point, that can be set to the origin without loss of generality. However several coplanar toes have different orientations that need to be taken into account in our model. With this consideration in mind, we embed in (8) an additional rotation term, $u_0 \in [0, 2\pi]$. Note that $u_0$ is not a control but this little abuse of notation allows to rewrite (8) in the more general form

$$\begin{cases} x_k = x_{k-1} + l_k e^{-i \sum_{h=0}^{k} u_h \ \omega} \\ x_0 = 0 \end{cases} \tag{21}$$

Note that if $u_1 = 0$, then $x_1 = l_1 e^{-i\omega u_0}$. The reachable set in time $k$ of this new system, $R_k^0$, reads

$$R_k^0 = \left\{ \sum_{j=1}^{k} l_j e^{-i\omega \sum_{h=0}^{j} u_h} \mid u_h \in U \right\} = e^{-i\omega u_0} R_k.$$

and, similarly,

$$R_\infty^0 = \left\{ \sum_{k=1}^{\infty} l_k e^{-i\omega \sum_{h=0}^{j} u_h} \mid u_h \in U \right\} = e^{-i\omega u_0} R_\infty.$$

**Remark 4.** In order to construct the reachable sets $R_k^0$ and $R_\infty^0$, Theorem 3.2 can be directly applied by considering the IFS $(F_u^0)$, where $F_u^0(x) := e^{-i\omega(u_0+u)}(Ax+B)$.

4.2. **Zygodactyl bird's foot.** The junctions of every finger are coplanar, we denote $p_i$, with $i = 1, \dots, 4$, the plane the $i$-th finger belongs to. All the planes of the fingers are assumed to be orthogonal to the $xy$-plane and we call $\Omega_i$, with $i = 1, \dots, 4$, the angle the plane $p_i$ forms with $xz$-plane. The condition $\Omega_1 = \Omega_3$ and $\Omega_2 = \Omega_4$ ensures Finger 1 and Finger 3 (and Finger 2 and Finger 4) to be coplanar, respectively. In Figure 2, $\Omega_1 = \Omega_3 = \pi/12$ and $\Omega_2 = \Omega_4 = -\pi/12$.

The initial rotation $u_0^i$ of the $i$-th finger is set to

0 for $i = 1, 3$, while for $u_0^2 = u_0^4 = \pi$. All fingers have in common their first junction, that, for seek of simplicity, coincides with the origin. We assume all fingers to have scale according to the same LCR sequence $(l_k)$ and to have the same maximal rotation angle $\omega$ and the same control set $U$.

We discuss the reachability of Finger 3, the other cases being similar. By Theorem 3.2 (see also Remark 4) the reachable set of the extremal junction of Finger 3, $R_4^3$, can be obtained by following algorithm

1. consider the LCR sequence of lengths $(l_k)$ with recursion depth $n \geq 0$ and set $u_0 := \Omega_3/\omega$.
2. iterate 4 times the IFS $\mathcal{F} = \{e^{-i\omega(u+u_0)}Ax + B, x \in \mathbb{C}, u \in U\}$ with initial datum $\{0\}$;
3. project the resulting $n$-dimensional set on its first component;
4. apply the isomorphism between $\mathbb{C}$ and $\mathbb{R}^3 \cap xz$-plane given by $x+iz \mapsto (x, 0, z)$.

See Figure 3 for some examples.

4.3. **Perching on a branch.** We consider the ability of our model bird's foot to grasp a branch, modeled as a cylinder. We discuss the case of coplanar fingers, say Finger 1 and Finger 3, so that the problem can be set on the complex plane

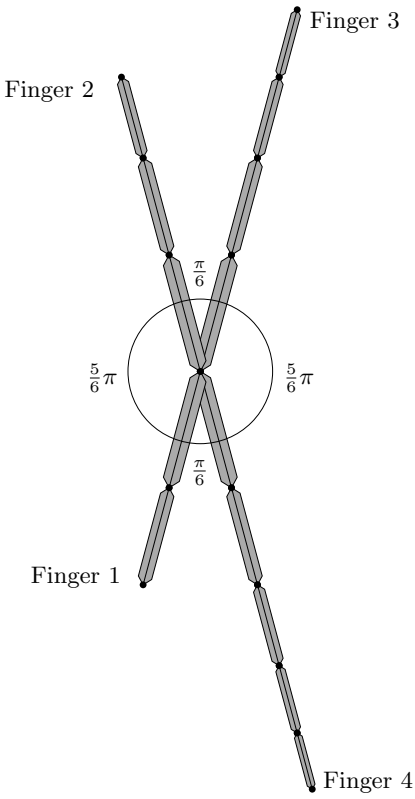


FIGURE 2. An example for our model: here $l_k = (1.2)^{-k}$. Note that the motions of Finger 1 and Finger 3 are coplanar, as well as for Finger 2 and Finger 4.

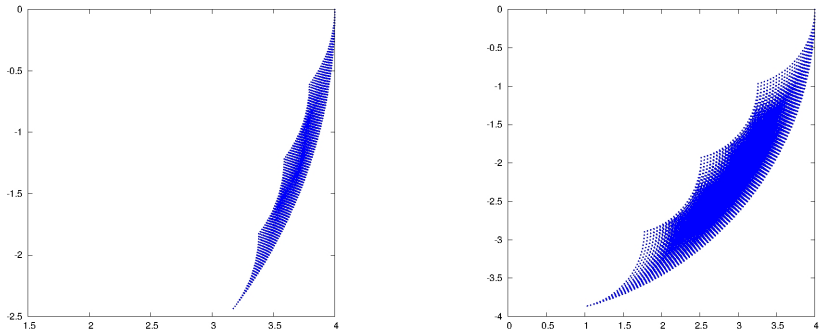

(A) $\omega = \pi/12$ (B) $\omega = \pi/6$

FIGURE 3. An approximation of the reachable set for Finger 3 $R_4^3$ with $\omega = \pi/12, \pi/6$ and $l_k = 1/\varphi^k$, where $\varphi$ is the Golden Mean, obtained by an uniform discretization of the control set $R = [0, 1]$. The consistency of this approximation is given by the continuity in Hausdorff metric of the attractor of $\mathcal{F}$ with respect to $R$ - see [15].

and reduces to consider the problem of grasping an appropriate ellipse, namely the section of the cylinder-branch related to the plane $p^1 (= p^2)$ - see Figure 4.

The ellipse $E$ generated by the intersection of a cylinder (with axis parallel to $y$-axis) and $p^1$ has a generic center of the form $(0, c_y)$ and radii of the form $(r\Omega_1, r)$. It can be parametrized as follows

$$x(\theta; c_y, r) = r\cos(\Omega_1)\cos(\theta)$$
$$y(\theta; c_y, r) = c_y + r\sin(\theta)$$

and its tangent vector given by is

$$\dot{x}(\theta; c_y, r) = -r\cos(\Omega_1)\sin(\theta)$$
$$\dot{y}(\theta; c_y, r) = r\cos(\theta)$$

Using the classical isomorphism $(x, y) \mapsto x + iy$ the ellipse on the complex plane may be parametrized by

$$\gamma(\theta; c_y, r) = c_y + r(\cos(\Omega_1)\cos(\theta) + i\sin(\theta)).$$

Grasp modeling is a deeply investigated topic in robotics and, in particular, a wide literature is devoted to the grasp of planar manipulators. In what follows we borrow from robotics some terminology and techniques in order formalize grasping conditions and the quality of the resulting grasp. In our setting, we assume that the fingers of the bird touch the surface of the branch (namely some phalanxes are tangent to the boundary of the ellipse $E$) in a finite number of contact points, $\mathbf{p}_1, \ldots, \mathbf{p}_n$. The unit normal vectors (with respect to $\partial E$) are denoted by $\mathbf{n}(\mathbf{p}_1), \ldots, \mathbf{n}(\mathbf{p}_n)$. The fingers exert on every contact point $\mathbf{p}_k$ a frictionless contact force $\mathbf{f}_k$, also termed *squeezing force*, whose magnitude is denoted by $f_k \geq 0$. Formally one has

$$\mathbf{f}_k = f_k \mathbf{n}(\mathbf{p}_k) \qquad \forall k = 1, \ldots, n.$$

Note that the condition $f_k \geq 0$ for every $k = 1, \ldots, n$, implies that $\mathbf{f}_1, \ldots, \mathbf{f}_n$ are pointing inward the branch. Every grasp is associated with the so-called *wrench system* $\{\mathbf{w}_1, \ldots, \mathbf{w}_n\}$, a subset of $\mathbb{R}^4$ containing the information related to the acting forces and torques. Formally the wrench $\mathbf{w}_k$ associated to the $k$-th contact point $\mathbf{p}_k$ of a planar manipulator reads

$$\mathbf{w}_k = (\mathbf{n}(\mathbf{p}_k), \mathbf{p}_k \times \mathbf{n}(\mathbf{p}_k)) \in \mathbb{R}^4$$

where $\times$ denotes the vector product. We consider a very simple grasp condition, commonly termed *force closure*.

**Definition 4.1.** A system of wrenches $\mathbf{w}_1, \ldots, \mathbf{w}_n$ is said to be a *force/torque closure grasp* if and only if any arbitrary external wrench can be generated by varying the magnitude of the wrenches. In other words, the positive space spanned by $\mathbf{w}_1, \ldots, \mathbf{w}_n$ is the entire $\mathbb{R}^4$. Equivalently one has the condition

$$\mathbf{0} \in int\ conv(\mathbf{w}_1, \ldots, \mathbf{w}_n). \tag{22}$$

In general, a planar force closure configuration requires four contact points. However when sacrificing the torque closure, three contact points are sufficient to achieve a force closure. This is the setting we shall consider. In other words, we are looking for three contact points $\mathbf{p}_1, \mathbf{p}_2, \mathbf{p}_3 \in \partial E$ such that

1. **Torque equilibrium condition.** The lines emanating from $\mathbf{p}_1, \mathbf{p}_2$ and $\mathbf{p}_3$ and following positively the corresponding directions$\mathbf{n}(\mathbf{p}_1)$, $\mathbf{n}(\mathbf{p}_2)$ and $\mathbf{n}(\mathbf{p}_3)$ are concurrent, namely they intersect in a single point.

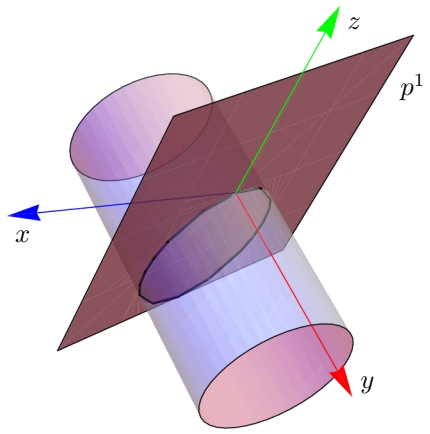


FIGURE 4. The cylinder represents a branch and it has radius 1 and axis $x = 0,\ z = -1$. The plane $p^1$ is the plane Finger 1 and Finger 3 belong to. The black ellipse is the intersection between $p^1$ and the boundary of the cylinder-branch.

2. **Force closure condition.** The unit inner normals $\mathbf{n}(\mathbf{p}_1)$, $\mathbf{n}(\mathbf{p}_2)$,$\mathbf{n}(\mathbf{p}_3)$ positively span the two-dimensional force space, namely for every $\mathbf{w} \in \mathbb{R}^2$ there exist $f_1, f_2, f_3 \geq 0$ such that

$$\mathbf{w} = \sum_{k=1}^{3} f_k \mathbf{n}(\mathbf{p}_k)$$

We aim to describe the possible branches (i.e. cylinders) that can be grasped by a couple of fingers. To this end, we first need to establish geometric conditions characterizing the contact points.

**Lemma 4.2.** *Consider a finger whose number of phalanxes is $K$. Let $u \in \{0,1\}^K$ be a control sequence and $x_k[u]$ the corresponding configuration. Also consider*

$$\phi_k(t) := x_{k-1} + t l_k e^{-i \sum_{j=0}^{k} u_j \omega}.$$

*Then a point $\mathbf{p} = (p_1, p_2) \in \mathbb{R}^2$ is a contact point between the ellipse $E$ and the finger if*

$$p_1 + i p_2 = \phi_k(t; u) = \gamma(\theta; c_y, r)$$

*where $k = 1, \ldots, K$ and $t \in [0,1]$ respectively ensure the existence of a solution and solve of the following system of equations*

$$\begin{cases} \phi_k(t;u) = \gamma(\theta; c_y, r) \\ \arg(\phi_k^{(h)}(t;(u_k))) = \arg(\dot{\gamma}(\theta; c_y, r)) \\ \theta \in [0, 2\pi),\ t \in [0,1] \end{cases} \tag{23}$$

*Proof.* The proof immediately follows by noticing that $\phi_k(t)$ is a parametrization on the complex plane of the $k$-th finger on the finger and the equations of (23) respectively are an incidence and a tangency conditions between the $k$-th phalanx and the section of the branch $E$. □

Next result summarizes above reasonings.

**Proposition 3.** *The bird's foot can grasp on a cylinder of center $c$ and radius $r$ using Finger 1 and Finger 3 if there exist two control sequences $(u_{k\leq K_h}^{(h)})$, with $i = 1, 3$ and $K_1 \leq 2$ and $K_3 \leq 4$, such that:*

*i) The system*

$$\begin{cases} \phi_k^{(h)}(t;u) = \gamma(\theta; c_y, r) \\ \arg(\phi_k^{(h)}(t;(u_k))) = \arg(\dot{\gamma}(\theta; c_y, r)) \\ \theta \in [0, 2\pi),\ t \in [0,1], k = 1, \dots, 3, h = 1, 3 \end{cases} \tag{24}$$

*admits at least three solutions $(k_j, h_j, t_j, \theta_j)$ with $j = 1, \dots, 3$, yielding the three contact points $\mathbf{p}_1 = \gamma(\theta_1; c_y, r)$, $\mathbf{p}_2 = \gamma(\theta_1; c_y, r)$ and $\mathbf{p}_3 = \gamma(\theta_1; c_y, r)$, according to the relation established in Lemma 4.2*

*ii) The torque equilibrium condition is satisfied, namely, there exist a solution for the system*

$$\begin{cases} \mathbf{p}_1 + \alpha_1 \mathbf{n}(\mathbf{p}_1) = \mathbf{p}_2 + \alpha_2 \mathbf{n}(\mathbf{p}_2); \\ \mathbf{p}_1 + \alpha_1 \mathbf{n}(\mathbf{p}_1) = \mathbf{p}_3 + \alpha_3 \mathbf{n}(\mathbf{p}_3); \\ \alpha_1, \alpha_2, \alpha_3 \geq 0 \end{cases}$$

*Above equations can be explicitly rewritten as*

$$\begin{cases} \gamma(\theta_1; c_y, r) + \alpha_1 \dot{\gamma}(\theta_1; c_y, r) = \gamma(\theta_2; c_y, r) + \alpha_2 \dot{\gamma}(\theta_2; c_y, r); \\ \gamma(\theta_1; c_y, r) + \alpha_1 \dot{\gamma}(\theta_1; c_y, r) = \gamma(\theta_3; c_y, r) + \alpha_3 \dot{\gamma}(\theta_3; c_y, r); \\ \alpha_1, \alpha_2, \alpha_3 \geq 0. \end{cases}$$

*iii) The force closure condition is satisfied, namely for every $\mathbf{w} \in \mathbb{C}$ there exist $f_1, f_2, f_3 \geq 0$ such that*

$$\mathbf{w} = \sum_{k=1}^{3} f_k \mathbf{n}(\mathbf{p}_k).$$

So far we did not take into account any constraint on the intensities of finger forces. This approach suffers of a lack of realism, since we are allowing arbitrary large forces. However, the results of Proposition 3 also hold when a constraint $\chi(f_1, f_2, f_3) = 1$ on the forces is imposed, by slightly modifying the force closure condition as follows: for every $\mathbf{w} \in \mathbb{C}$ there exist $f_1, f_2, f_3$ such that $\chi(f_1, f_2, f_3) = 1$ and

$$\mathbf{w} = \sum_{k=1}^{3} f_k \mathbf{n}(\mathbf{p}_k).$$

This generalization makes more interesting the equivalent force closure condition: there exists $R > 0$ such that the ball of radius $R$ and centered in the origin $B_r$ satisfies

$$B_R \subset conv \left\{ \sum_{k=1}^{3} f_k \mathbf{n}(\mathbf{p}_k) \mid \chi(f_1, f_2, f_3) = 1 \right\}. \tag{25}$$

The maximal radius $r$ satisfying above inclusion gives a measure of the quality of the grasp [20]. Indeed it can be showed that the larger is $r$, the strongest is the capability of the grasp to resist at external forces or, in the case of force/torque closure, to external wrenches. We then conclude our reasoning on the grasping with the following

(3) **Optimality condition.** Let $\theta_1, \theta_2, \theta_3 \in [0, 2\pi]$ and assume $\mathbf{p}_k = \gamma(\theta_k, C_y, R)$, $k = 1, \dots, 3$, be three contact points between the branch and two fingers of bird's foot. Assume the corresponding grasp to be force closure, according to Proposition 3. Then the grasp is optimal if

$$(\theta_1, \theta_2, \theta_3) = \arg\max \{R \mid B_R \subset G_\chi\}$$

where

$$G_\chi := conv \left\{ \sum_{k=1}^{3} f_k \mathbf{n}(\mathbf{p}_k) \mid \chi(f_1, f_2, f_3) = 1 \right\}.$$

4.4. **Tendon locking mechanism in owl's foot.** Owls have zygodactyl feet ensuring a good grasp when perching or clutching a pray. They are characterized by the further ability of rotating the a third toe to the front when in flight - see Figure 5. In particular, when attacking the pray, the talons are spread out wide to increase the chance of a successful strike. Owl's feet are also endowed with the so called digital Tendon Locking Mechanism (TLM), common among bats too. When an object, say a perch or a pray, touches the base of the foot then TLM engages and keeps the toes locked around the object without the need for the muscles to be contracted [24].

From a mathematical point of view, TLM can be modeled as an hybrid system: when the first phalanx of any toe, namely the base of the foot, is not in contact with an object then the position of the phalanxes evolves according the control dynamics described in previous section. If otherwise the first phalanx belongs to an appropriate region of $\mathbb{R}^3$ denoted by $\mathcal{O}$ and representing an obstacle, say a pray or a branch, then TLM engages. Since TLM is not a voluntary movement, then the corresponding dynamic is not controlled - see Figure. 5-(A).

(A) Zygodactyl configuration (B) Isodactil configuration

FIGURE 5. Owl's foot in two configurations, (A) is suitable for grasping, (B) is the typical flight configuration: as soon as a pray is targeted, phalanxes spread wide in order to maximize the chance of grabbing it.

As in previous sections, let $x_k^{(h)}$ be the position of the $k$-th junction of the $h$-th toe of owl's foot and $u_k^{(h)} \in [0, 1]$ be the corresponding rotation control. In our model phalanxes are segments, in particular the first phalanx of the $h$-th toe is the set

$$P^{(h)} := \left\{ a x_1^{(h)} \mid a \in [0, 1] \right\}.$$

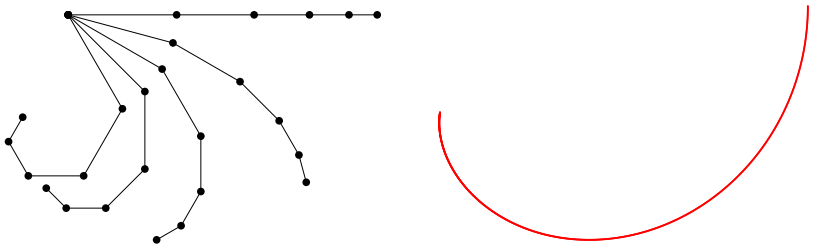

(A) TLM engagement for Finger 4

(B) Talon (i.e. extremal of the toe) trajectory

FIGURE 6. Various stages of TLM engagement: all rotational controls are equal to $v(t) \in [0, \pi/6]$, $t \in [0, T]$, where $T$ is engagement time.

Also define the TLM map $v(t) : [0, T] \mapsto [0, 1]$ where $T$ is the is the engagement time, that is the time requested to the toes to contract when it touches an object $\mathcal{O}$, and $v(t)$ is a continuous non-decreasing map. We have for every $h = 1, \dots, 4$

$$\begin{cases} x_k^{(h)}(t) = \sum_{j=1}^{k+1} l_j e^{-i\omega \sum_{n=1}^{j} u_n^{(h)}(t)} & \text{if } P^{(l)} \cap \mathcal{O} = \emptyset; l = 1, \dots, 4 \\ x_k^{(h)}(t) = \sum_{j=1}^{k+1} l_j e^{-i\omega j v(t)} & \text{otherwise} \end{cases} \tag{26}$$

**Remark 5.** If $\mathcal{O}$ is convex then $P^{(l)} \cap \mathcal{O} \neq \emptyset$ for some $l = 1, \dots, 4$ is satisfied for every $t \in [0, T]$. At time $T$ the tendon is locked and no further movement is allowed. This is indeed the goal of such mechanism: to keep the toes contracted without the contribution of muscles. We postpone the investigation of models for the TLM disengagement in a future work.

## REFERENCES


[1] J. Baillieul, Avoiding obstacles and resolving kinematic redundancy, *IEEE International Conference on Robotics and Automation,* **3** (1986), 1698–1704.

[2] M. F. Barnsley, *Fractals Everywhere: New Edition*, Courier Dover Publications, 2013.

[3] M. F. Barnsley and K. Leśniak, On the continuity of the Hutchinson operator, preprint, arXiv:1202.2485, 2012.

[4] W. J. Bock, Functional and evolutionary morphology of woodpeckers, *Ostrich,* **70** (1999), 23–31.

[5] J. W. Burdick, *Kinematic Analysis and Design of Redundant Robot Manipulators,* Diss. Stanford University, 1988.

[6] G. S. Chirikjian and J. W. Burdick, An obstacle avoidance algorithm for hyper-redundant manipulators, *IEEE International Conference on Robotics and Automation*, **1** (1990), 625–631.

[7] G. S. Chirikjian and J. W. Burdick, The kinematics of hyper-redundant robot locomotion, *IEEE Transactions on Robotics and Automation,* **11** (1995), 781–793.

[8] Y. Chitour and B. Piccoli, Controllability for discrete systems with a finite control set, *Mathematics of Control, Signals and Systems,* **14** (2001), 173–193.

[9] N. Dubbini, B. Piccoli and A. Bicchi, Left invertibility of discrete systems with finite inputs and quantised output, *International Journal of Control,* **83** (2010), 798–809.

[10] J. Hutchinson, Fractals and self-similarity, *Indiana Univ. J. Math.,* **30** (1981), 713–747.

[11] E.-U. Imme and G. S. Chirikjian, Inverse kinematics of discretely actuated hyper-redundant manipulators using workspace densities, in *Proceedings of 1996 IEEE International Conference on Robotics and Automation. Vol. 1*, IEEE, 1996, 139–145.
[12] P. Glendinning and N. Sidorov, Unique representations of real numbers in non-integer bases, *Mathematical Research Letters,* **8** (2001), 535–543.
[13] V. Komornik, A. C. Lai and M. Pedicini, Generalized golden ratios of ternary alphabets, *J. Eur. Math. Soc.,* **13** (2011), 1113–1146.
[14] V. Komornik and P. Loreti, Unique developments in non-integer bases, *American Mathematical Monthly*, **105** (1998), 636–639.
[15] A. C. Lai and P. Loreti, Robot's finger and expansions in non-integer bases, *Networks and Heterogeneus Media,* **7** (2012), 71–111.
[16] A. C. Lai and P. Loreti, From discrete to continuous reachability for a robot's finger model, *Communications in Industrial and Applied Mathematics,* **3** (2012), e-439, 22pp.
[17] M. D. Lichter, V. A. Sujan and S. Dubowsky, Computational issues in the planning and kinematics of binary robots, in *Proceedings of ICRA'02 IEEE International Conference on Robotics and Automation. Vol. 1,* IEEE, 2002, 341–346.
[18] L. Mederreg, et al., *The RoboCoq Project: Modelling and Design of Bird-like Robot,* 6th International Conference on Climbing and Walking Robots, CLAWAR, 2003.
[19] A. Mihail and R. Miculescu, The shift space for an infinite iterated function system, *Math. Rep. (Bucur.),* **11** (2009), 21–32.
[20] B. Mishra, *Grasp Metrics: Optimality and Complexity,* Proceedings of the Workshop on Algorithmic Foundations of Robotics, AK Peters, Ltd., 1995.
[21] R. Norberg, Treecreeper climbing, mechanics, energetics, and structural adaptations, *Ornis Scandinavica,* (1986), 191–209.
[22] M. Pedicini, Greedy expansions and sets with deleted digits, *Theoretical Computer Science,* **332** (2005), 313–336.
[23] Y. Peres, M. Rams, K. Simon and B. Solomyak, Equivalence of positive Hausdorff measure and the open set condition for self-conformal sets, *Proceedings of the American Mathematical Society,* **129** (2001), 2689–2699.
[24] T. Quinn and J. Baumel, The digital tendon locking mechanism of the avian foot (Aves), *Zoomorphology*, **109** (1990), 281–293.
[25] N. A. Secelean, *Masura si Fractali,* Univ. Lucian Blaga, Sibiu, 2002.
[26] D. Sustaita, et al., *Getting a Grip on Tetrapod Grasping: Form, Function, and Evolution,* Biological Reviews, **88** (2013), 380–405.
[27] A. V. Zinoviev and F. Ya Dzerzhinsky, Some general notes on the avian hindlimb biomechanics, *Bulletin of Moscow Society of Naturalists,* **105** (2000), p5.

Received September 2014; revised December 2014.

*E-mail address*: anna.lai@sbai.uniroma1.it
*E-mail address*: paola.loreti@sbai.uniroma1.it